Crystal dynamics of nitrogen: The cubic α-phase

J. K. Kjems*

Brookhaven National Laboratory,† Upton, New York 11973

G. Dolling‡

Atomic Energy of Canada Limited, Chalk River Nuclear Laboratories, Chalk River, Ontario KOJ 1JO

The technique of inelastic neutron scattering has been used to determine translational and librational lattice modes in a single crystal of solid nitrogen in the cubic α-phase at 15 K. The measurements were concentrated at the high-symmetry points Γ, R, and M, where the degeneracies ease the task of symmetry assignments to the observed modes. The assignment was made on the basis of the correlation of the observed structure-factor variation with force-model predictions. The calculations were based on a general potential function which includes Lennard-Jones or six-exponential-type interactions as well as electric quadrupole forces. Good agreement was found between both the observed frequencies and the observed intensities and their calculated counterparts. The temperature dependence of selected modes has been established and it is compared to a recent self-consistent phonon calculation.

I. INTRODUCTION

During the past several years, a considerable number of experimental and theoretical studies have been made of molecular motions and intermolecular potentials in simple molecular materials with linear molecules, such as solid nitrogen. Much of this work has involved the measurement of the frequencies of the optically active intermolecular modes by means of far-infrared[1,2] and Raman[3,4] spectroscopy, and the establishment of various theoretical force models[5-10] to describe the experimental results. Raman scattering measurements have also been made[11,12] of the temperature and pressure dependence of certain modes in the various solid phases of N_2. The application of the techniques of thermal-neutron coherent inelastic scattering to these molecular-dynamics problems is a recent development: Such experiments have been performed on solid hydrogen[13] and carbon dioxide.[14] The advantage of the neutron scattering method, at least in principle, is that normal modes of any wave vector $\vec{q}$ throughout the Brillouin zone may be studied, whereas optical techniques are restricted to a limited number of modes of essentially zero wave vector.

In this paper we describe neutron inelastic scattering experiments made on single-crystal specimens of solid nitrogen, with the aid of triple-axis crystal spectrometers[15] at the Brookhaven High Flux Beam Reactor. Solid N_2 at ordinary pressure exists in two phases: a low-temperature cubic α-phase which is the stable form below 35.6 K, and a hexagonal β-phase which exists between 35.6 K and the melting point at 63.2 K. There is also a tetragonal γ-phase at high pressure.[16,17] The space group of α-N_2 is believed[12] to be $P2_13(T^4)$, although the centers of the four N_2 molecules within each

unit cell lie very closely on an fcc lattice, corresponding to the structure $Pa3(T_h^6)$. Furthermore, the bulk of the spectroscopic evidence (e.g., selection rules) favors the latter space group; there are only slight indications of coincidences between Raman and infrared lines. It therefore seems reasonable to assume the more symmetric structure in the interpretation of the neutron scattering results. In any event, in the α-phase, the four molecules are aligned along four different [111] directions, as indicated in Fig. 1. The α-β phase change at 35.6 K involves a shift of the molecular centers from the face-centered-cubic arrangement to a hexagonal-close-packed one; the molecular orientation is no longer well defined; the molecules are probably switching rapidly between a number of possible orientations,[18,19] in contrast to the relatively small oscillations about fixed equilibrium orientations characteristic of the α-phase.

The format of the paper is the following: In Sec. II we describe the specimen preparation, the experimental conditions, and the types of measurements made; the results for the α-phase, including the temperature dependence of certain normal modes in the vicinity of the transition, are given in Sec. III. At temperatures well below the transition, the results indicate the existence of well-defined translational and librational (or mixed) modes qualitatively similar to those observed in solid carbon dioxide.[14] There is excellent agreement between the present measurements at the point Γ (wave vector $\vec{q} = 0$) and those previously obtained by optical techniques.[1-4,11,12] The implications of these results for theoretical models of the intermolecular forces are discussed in Sec. IV. Calculations are presented of normal modes in the α-phase, based on (a) empirical interatomic potentials of the Lennard-Jones and Buckingham analytic
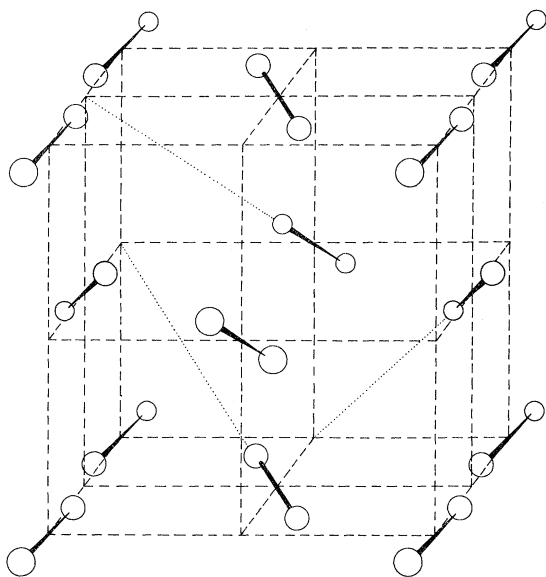
FIG. 1. Illustration of the $Pa3$ structure of the α-phase of solid N_2. The four molecules in the cubic unit cell occupy the face-centered position and the molecular axes point along the four body diagonals.

forms, and (b) a point-charge model for the electrostatic forces between the quadrupolar distribution of electrons in the nitrogen molecule. Finally, in Sec. V we discuss our results in the context of related work.

The results obtained for the hexagonal β-phase are in marked contrast to those for the α-phase. Broad energy distributions of scattered neutrons are observed at relatively high momentum transfer, where scattering from librational modes would be expected theoretically. Peaks corresponding to translational motions of the N_2 molecules are seen at low momentum transfers: These are reminiscent of the results for phonons in solid hydrogen[13] or in hexagonal-close-packed metals. In view of these differences from the α-phase, the results for the β-phase, and their interpretation, will be presented in a separate paper.

II. EXPERIMENTAL

A. Single-crystal specimens

A crystal of β-N_2 was grown by slow cooling of liquid nitrogen contained in a cylindrical cell mounted in a Cryogenics Associates liquid-helium cryostat. The cell, 1 cm diameter and 4 cm long, was made from a transparent plastic material (Kapton), and could be viewed optically through variable slits in the metal radiation shields of the cryostat. This particular sample-cell design has previously been used at Brookhaven for the study of rare-gas

solids.[20] Care was taken, during the growth and subsequent slow cooling of the crystal to 36 K, to maintain a temperature gradient, about 1 K/cm, along its length. This appeared to reduce the chance of cracking the solid. The mosaic spread full width at half-maximum (FWHM) of the single crystal, initially $< 0.2°$, increased steadily to $\sim 1°$ during cooling. The crystal was maintained at a uniform temperature of 36 K for several days while experiments on the β-phase were carried out. Finally, the crystal was very slowly cooled, over a period of 3 to 4 h, through the phase transition at 35.6 K. Certain Bragg reflections of the hexagonal phase and of the expected cubic phase were checked every few minutes during this time to follow the progress of the transition. Hexagonal reflections such as (0002), which have an analogous reflection with the same d spacing in the cubic phase, showed a steady decrease in intensity, eventually reaching a level about half their original strength. At the same time, other reflections, such as ($10\bar{1}0$), decreased to zero intensity. When all the material had transformed into the α-phase, it was found by means of Bragg-reflection photographs to consist of one single crystal, about 1.5 cm^3 in volume, i.e., one half of the total, surrounded by many small disoriented fragments. The orientation of the large crystal corresponded with that of the initial β-phase crystal: the [111] and [$0\bar{1}1$] cube axes being parallel to the initial [0002] and [11$\bar{2}$0] hexagonal axes. The mosaic spread was about 1° (FWHM). In the subsequent α-phase experiments the neutron beams were stopped down so that scattering predominantly occurred in the large crystal.

B. Spectrometer arrangement and types of scan

Experiments were performed with three different spectrometer configurations: (i) incident neutron energy fixed at 13.5 meV, scattered neutron energy variable within the range 15.0–5.0 meV; (ii) incident neutron energy fixed at 30 meV, scattered neutron energy variable, 30–20 meV; and (iii) scattered neutron energy fixed at 13.5 meV, incident neutron energy variable, 12–25 meV. In all cases, the (0002) planes of a curved pyrolitic graphite crystal were used as monochromator, with a flat pyrolitic graphite crystal as analyzer. The "constant-$\vec{Q}$" mode of operation[15] was used throughout. Most of the experiments were performed with 20' and 40' Soller slit collimators both before and after the monochromator and analyzer crystals, respectively. Configuration (i) was used to measure the low-energy excitations, mostly in the range 0 to 5 meV, with an over-all energy resolution of about 0.4 meV, while configuration (ii) allowed observation of the higher-energy modes with good intensity but relatively poor resolution (about 2.0 meV). For
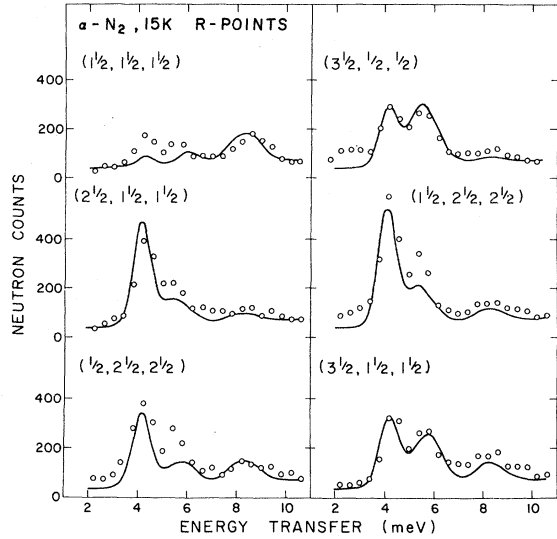
FIG. 2. Examples of inelastic scans at the R point ($\frac{1}{2}$, $\frac{1}{2}$, $\frac{1}{2}$) in various zones at 15 K. All the scans were made under identical experimnetal conditions, with a counting time of 5 min per point. The full curves are the calculated responses for all five normal modes taking into account instrumental corrections and estimated intrinsic widths as explained in the text.

scans over the whole energy range of interest, at the points Γ, R, and M of high symmetry in the Brillouin zone, the most satisfactory configuration was found to be (iii), since this automatically allows the resolution to decrease, and hence the scattered intensity to increase, to compensate for the reduced cross section for the higher-energy modes. Figure 2 shows several constant-$\vec{Q}$ scans taken in this way, at 15 K, for neutron-momentum-transfer vectors $\vec{Q}$ corresponding to the R point (0.5, 0.5, 0.5). A typical counting time for one such scan was 5 min per

point. The observed widths of those peaks which are reasonably well separated from each other are in the range 0.8 to 1.5 meV; this is somewhat larger than the widths to be expected from the energy resolution alone. The broadening is partly due to the intrinsic lifetime of the observed excitations and partly due to the dispersion at small wave vectors away from the R points which is sensed via the finite wave-vector resolution.

At a general wave vector $\vec{q}$ within the Brillouin zone, the experimental situation is quite complex, since as many as 20 distinct modes may contribute to the spectrum of scattered neutrons, and the resolution of the neutron spectrometer is inadequate to distinguish all these contributions. However, at the high-symmetry points Γ, R, and M, and also for acoustic modes propagating in various directions, where only a few distinct modes are expected, it is possible to measure the frequencies of these modes. Even then the problem may be complicated by the occurrence of near degeneracies as illustrated by Fig. 2. There we show the observed intensities at the R point in various zones. There are five distinct R-point frequencies but the data never show more than three peaks. Close examination reveals that the two lower-frequency peaks are shifted slightly in going from one zone to the other, indicating that they are composed of two overlapping lines. The identification and assignment of the modes can be accomplished by comparing the observed intensities of the various peaks with those calculated from normal-mode eigenvectors derived from a suitable intermolecular force model. In fact, this is a kind of iterative process, in which one first establishes a force model having a number of adjustable parameters, and then adjusts these parameters until both the mode frequencies and the intensities in various zones, calculated from the model, are in agreement with experiment. We shall discuss this problem in more detail in Sec. IV.

TABLE I. Lattice-mode frequencies in α-N_2 at 15 K (meV).

	A_u/Γ_1^-	E_u/Γ_{23}^-	T_u/Γ_4^-	E_g/Γ_{23}^+	T_g/Γ_4^+
Observed	5.8 ± 0.2	6.7 ± 0.3	$6.0 \pm 0.1; 8.6 \pm 0.2$	4.0 ± 0.1	$4.5 \pm 0.1; 7.4 \pm 0.2$
Calculated[a]	5.72	6.11	5.65 ; 8.24	3.76	4.84 ; 7.53
	R_1^-	R_{23}^-	R_{23}^-	R_1^+	R_{23}^+
Observed	4.2 ± 0.1	4.3 ± 0.1	8.5 ± 0.2	5.4 ± 0.2	5.85 ± 0.2
Calculated[a]	3.96	4.16	8.11	5.15	5.83
	All M_{12} modes				
Observed	3.45 ± 0.15	4.70 ± 0.2	5.8 ± 0.2	6.8 ± 0.2	7.75 ± 0.2
Calculated[a]	3.76	5.03	5.65	6.41	7.01

[a]Calculations based on model I; see Sec. IV and Table III.

TABLE II. Elastic constants of α-N_2 at 15 K (10^{10} dyn$\cdot$cm^{-2}).

C_{11}	2.90 ± 0.05
C_{12}	2.00 ± 0.10
C_{44}	1.35 ± 0.05
$B = (C_{11} + 2C_{12})/3$	2.3 ± 0.2
B(obs., Ref. 21)	2.13

III. EXPERIMENTAL RESULTS

Scattered neutron energy distributions, similar to those shown in Fig. 2, were measured at 15 K at the high-symmetry points Γ, R, and M, in many different zones. From these we have deduced values for the frequencies of the 17 distinct modes corresponding to these wave vectors, as shown in Table I. We have also measured, at 15 K, the dispersion curves for certain acoustic modes propagating along the three principal symmetry directions Δ, Σ, and Λ. From the initial slopes of these curves, after small corrections for resolution effects, we can deduce the three elastic constants for α-N_2. These are given in Table II, and compared with the independently measured compressibility.[21]

Certain scans, showing well-defined peaks corresponding to selected normal modes, were measured at three higher temperatures (24, 30, and 34.5 K), in an attempt to correlate the α-β phase transition at 35.6 K with the temperature dependence of the modes. Two examples, namely, the results for the E_g and T_g zone-center modes, are
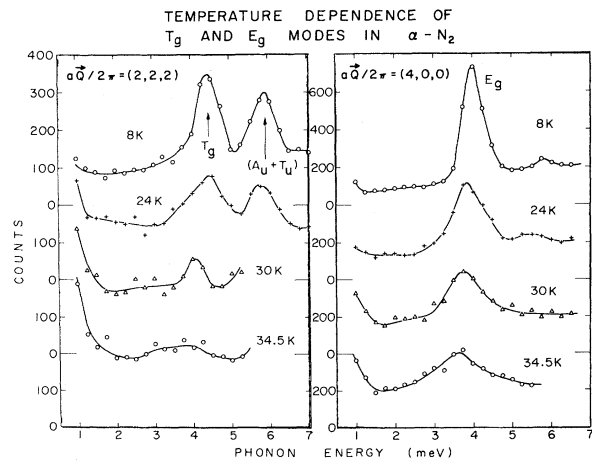
shown in Fig. 3. In almost all cases, the neutron groups, initially well defined at 15 K, decreased slowly in frequency and showed appreciable broadening; the results for the E_g mode seen at the (4,0,0) reciprocal-lattice point, Fig. 3, is typical. Of the modes studied to date in this way, only the lower T_g mode displayed any more striking behavior, Fig. 3. The broadening is so marked in this case that at 34.5 K the peak has almost disappeared, leaving a broad spectrum of intensity extending to quite low energies. The observed peak positions are plotted against temperature in Fig. 4 and again it is the lower T_g mode that shows the most dramatic change.

IV. FORCE MODELS

A. Introduction

The several existing theoretical models[5-10] for the intermolecular forces in α-N_2 have all been compared with, and in some cases fitted to, the frequencies of the optically active modes at Γ. Some of the models[6,8] have dealt only with the librational modes, by considering the molecular centers to be rigidly fixed at the face-centered cubic positions. Others[5,10] have attempted to calculate all the normal-mode frequencies on the basis of either a Lennard-Jones type of atom-atom potential or a quadrupole-quadrupole potential (but not both together), while a third approach[3] has been to em-

TEMPERATURE DEPENDENCE OF
T_g AND E_g MODES IN α-N_2

FIG. 3. Temperature dependence of the inelastic neutron scattering at two Γ points where the E_g and the lower T_g modes are seen well isolated. The lines through the measured points are merely guides to the eye.
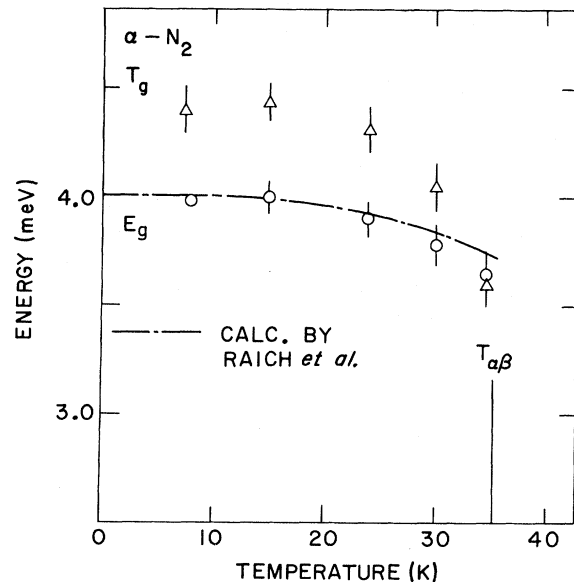

FIG. 4. Observed peak positions of the scans shown in Fig. 3. The line near the E_g mode is the result of a self-consistent phonon calculation by Raich et al. (Ref. 33) which has been normalized to the observed frequencies at low temperature.

ploy the quadrupole potential in conjunction with and "effective" Lennard-Jones potential between molecular centers. None of these approaches has proved to be entirely satisfactory, and it is apparent[10] that any improved model must include, at the very least, both repulsive and attractive "dispersive" potentials V_r, V_a between atoms on different molecules, and also the electrostatic interaction V_q between the molecular quadrupole moments. A rather simple model potential satisfying these minimum requirements–a model which does not appear to have been tried as yet for solid N_2–can thus be written

$$V = V_a + V_r + V_q , \tag{1}$$

where

$$V_a = -A r^{-6} + C r^{-8} + \cdots \tag{2}$$

and

$$V_r = +B e^{-\alpha r} \tag{3}$$

or

$$V_r = +D r^{-n} , \tag{4}$$

where n is usually taken to be 12 (Lennard-Jones) although there is evidence[10] that smaller values, as low as 9, may be more satisfactory from some points of view in the case of α-N_2. We have calculated the normal-mode frequencies of α-N_2 for several variants of the above model, with V_r represented either by (3) or (4), and B, D, and to a limited extent α and n, being considered as adjustable parameters. In all our calculations we have assumed, in Eq. (2), that $C = 0$ along with all higher-order terms, and that the quadrupolar distribution of electrons in one molecule can be represented by a charge Ze at each atom site and a charge $-2Ze$ at the center of the molecule. The resulting electrostatic energy and electrical intermolecular forces turn out to be similar to those which one would obtain from a point-quadrupole model. For example, the electrostatic force between a nearest-neighbor pair of N_2 molecules, regarded as extended charge distributions, is 6.3% less than if the molecules are represented by point quadrupoles with the same quadrupole moment. The electrostatic contributions to the various force constants, and hence to the librational-mode frequencies, show larger differences, however, as would be expected since these depend on higher derivatives of the potential. In this connection, we believe it may be more realistic to represent the electronic distribution around the molecule by a linear array of point charges than by a point quadrupole at the molecular center.

It should be emphasized that our calculations have so far been confined to the harmonic approximation;

this is believed[6] to be quite satisfactory for the translational modes, though much less so for the librational modes. However, if a qualitatively satisfactory harmonic model, including all the above-mentioned terms in a physically realistic manner, can first be established, it will then be appropriate to consider such refinements as higher-order terms in the potential [e.g., $C \neq 0$ in Eq. (2)] and anharmonic effects. Furthermore, a relatively simple but realistic model of this kind is most valuable, perhaps even essential, for the correct analysis and interpretation of the neutron inelastic scattering results, as mentioned in Sec. II B.

B. Method of calculation

The electrostatic forces between the arrays of point charges mentioned in Sec. IV A are expressed in terms of the so-called Coulomb coefficients,[22] which may be computed to high accuracy by means of the Ewald θ transformation. The only adjustable parameter in the calculation of V_q is thus the charge z. The dispersive forces are expressed in terms of the first and second derivatives of the potentials V_a, V_r, evaluated at the appropriate distances between the equilibrium positions of the nitrogen atoms on different molecules. All atom-atom bonds up to 7 Å in length were included in order to ensure substantially better than 1% accuracy in the calculated mode frequencies. The necessity of including these rather long "bonds" arises because of the long range of the van der Waals term V_a. Many previous calculations[23-26] of interatomic forces in molecular crystals have been carried out with the Buckingham-type potential (3). From a consideration of this work, it would appear that the value of α for nitrogen-nitrogen forces lies in the range 3.58–3.64 Å^{-1}. Within this range, we find that α and B are very closely correlated, an increase in α being almost precisely compensated by an appropriate increase in B. The potential is thus represented, in effect, by only one parameter, as is the Lennard-Jones potential (4) when n is fixed at 12.

The distance d between the nitrogen atoms in one molecule has been quoted variously as 1.055,[27] 1.098,[28] and 1.104 Å.[29] The second value, determined from Raman scattering measurements of the rotational band, appears to be the most precise, so we have used it in our force-model calculations.

The strong covalent N-N bond is formed by the sharing of electrons between the atoms, so that the electronic distribution extends over the whole length of the molecule rather than being concentrated only around the atom sites. In our simple model we represent the forces as acting between specific points (normally the nuclear positions), but since these forces arise from the electron clouds, it would be physically plausible to assume

that they act at points displaced along the bond in the direction of the center of the molecule. (The model of Anderson *et al.*[3] assumes a single point of interaction in the center.) We might thus speak of an "effective" bond length,[5] being the separation of the two points at which the interatomic forces are supposed to act, which is rather less than the actual atomic separation. Another physical property which may be taken into account by such an effective bond length is the large molecular libration amplitude. This has been estimated[6] to be as high as 20° and, from the viewpoint of the surrounding molecules, could give rise to an apparent reduction in bond length. (We should emphasize that in our effective-bond-length calculations of normal-mode frequencies, we ensure that the moment of inertia of the N_2 molecule is left unchanged.) A different method of taking these bond-reduction effects into account in our model might be to "soften" the repulsive potential (3) or (4) by reducing α or n, respectively. Whichever method is employed, it is easy to see that the major effect on the calculated phonon frequencies will be to lower the librational modes with respect to the translational modes. (If the effective bond length were reduced to zero, while maintaining the correct molecular mass and moment of inertia, then the librational-mode frequencies would tend to zero.) We shall see, however, that the most effective method of achieving a good fit to all the modes is by a reduction of the bond length rather than by reducing n or α.

In most of our model calculations, two constraints were applied in the form of additional "experimental data points" which the models were required to fit as closely as possible. There were (a) that the total potential energy of the crystal should be equal to the measured sublimation energy, after correction for the effect of zero-point energy of vibration and libration for the molecules, and (b) that the derivative of the total potential energy with respect to the lattice parameter should, in the absence of any externally applied pressure, be given by the thermal pressure. The latter constraint ensures that the crystal will have minimum energy at the observed lattice parameter ($a = 5.644$ Å).

The sublimation energy (the value 1.652 kcal/ mole has been quoted by Kohin[29]) is derived from the observed total heat required[30] to sublime 1 mole of solid N_2, initially at absolute zero, by subtracting the energy of the nitrogen gas ($7kT/2$) at 77.3 K. (The contribution of the internal energy of each molecule is of course neglected, and a small correction for non-ideal-gas behavior is also applied.) The contributions to the zero-point energy of the solid, arising from the librational and translational modes have been estimated to be 0.123 and 0.213,[29] or 0.126 and 0.184 kcal/mole,[6] respectively. From

these values we finally deduce that the total potential energy should be -1.990 ± 0.05 kcal/mole.

The second constraint, that of zero external stress at the observed lattice parameter, is difficult to calculate exactly, since it requires a knowledge of the variation with crystal volume of all the normal-mode frequencies, that is to say, the microscopic Grüneisen γ values. We have assumed an average γ value 1.81 for α-N_2; this is the weighted average of the γ values for the E_g and T_g modes measured by Medina and Daniels.[12]

C. Results of calculations

The initial calculations were carried out in a straightforward manner, with the effective molecular bond length assumed to be equal to the true bond length (1.098 Å). The charge Z on any nitrogen atom, the van der Waals parameter A, and *either B or D* (with $n = 12$) were varied by the method of least squares so as to produce the best fit to 17 selected normal-mode frequencies at 15 K (7 at Γ, 5 at R, and 5 at M) and also to the measured quadrupole moment.[31,32] Three different α values were used in turn, 3.58, 3.61, and 3.64, in fitting Buckingham potential (3) to the results. It was found that very similar fits were obtained for all three α values when the value of B was adjusted appropriately, with the lower α values providing somewhat better results. These fits were also very similar to those obtained with the Lennard-Jones potential (4), and it became clear that there was little to choose, from an experimental point of view, between these two repulsive potentials. To be more specific, let us define a (weighted) sum of squares

$$\chi^2 = \sum_{i=1}^{n} \frac{\rho_i [\nu_i^2(\text{calc}) - \nu_i^2(\text{obs})]^2}{n - p} \quad , \quad (5)$$

where $\rho_i = (2\nu_i \Delta_i)^{-2}$, $\nu_i \pm \Delta_i$ is the phonon frequency and its experimental error, and n, p are the numbers of observations and adjustable parameters, respectively. We were able to find only one minimum value of χ^2 within the parameter space, to which the fitting program returned no matter what starting parameter values were used. This minimum value was quite sharply defined in all cases. The results for the Lennard-Jones (L-J) and two of the Buckingham-type potentials are shown as models II, IV, and V in Table III. The most serious defect of all these models is that the frequencies of the modes at Γ ($q = 0$) are relatively poorly fitted. In particular, the upper T_g and upper T_u modes are calculated to be in reverse order. The same remark applies to the lower T_g and lower T_u modes. Thus, according to model II, these modes have calculated frequencies 7.77, 7.71 and 5.35, 5.28 meV, respectively, as compared with the observed

values 7.4, 8.6 and 4.5, 6.0 meV. The values for A_u, E_u, and E_g are also considerably in error (5.37, 5.85, and 4.36 meV, respectively). Even when very high weights were given to the modes, it proved impossible to achieve the correct ordering of the T_u and T_g frequencies. The same difficulty remained if the two constraints concerning the total energy and zero external stress were completely relaxed, or if the quadrupole moment was omitted from the fitting process. One significant effect of relaxing the constraints was noticed, however: The minimum of χ^2 in the parameter space becomes extremely shallow, so that a large number of almost equivalent (i.e., equally unsatisfactory) fits to the measured frequencies could be obtained over a wide range of values of A, B or A, D. It is clear that the phonon frequencies depend, through the potential derivatives, upon a certain function of the differences $A-B$ or $A-D$, rather than on the individual parameters. The application of the two additional constraints, particularly that concerning the total energy, has the beneficial result of fixing the individual values of A and B or of A and D.

Since it appeared unlikely that an improved fit could be achieved with any reasonable value of α, the effect of varying n, in Eq. (4), was tried. The result for $n = 10$ is shown as model III in Table III. The over-all quality of the fit is much the same as for model II, $n = 12$. Finally, a calculation was made based on the picture described in Sec. IV B, in which the effective center of force acting on one end of a molecule is located somewhat closer to the molecular center than the true nuclear position. The effective bond length is a basic input to the calculation, which cannot easily be treated as a variable parameter in a least-squares fit. We therefore chose an arbitrary effective bond length, 0.923 Å, 16% less than the true bond length, 1.098 Å. Care was taken in these calculations to maintain the correct molecular moment of inertia. The result of the fitting calculation is given as model I,

TABLE III. A selection of intermolecular force models for α-N_2 at 15 K. Units: A, 10^2 kcal/mole Å (Ref. 6); B (models IV, V), 10^4 kcal/mole; D (models I, II), 10^2 kcal/mole Å (Ref. 12); D (model III), 10^4 kcal/mole Å (Ref. 10).

Model: characteristics	$Z(e)$	A	B or D	χ
I[a]: L-J, $n = 12$	0.544	3.983	5.970	2.08
II: L-J, $n = 12$	0.353	3.575	4.544	4.41
III: L-J, $n = 10$	0.353	4.745	5.738	4.41
IV: 6-exp, $\alpha = 3.58$	0.371	3.192	3.827	4.49
V: 6-exp, $\alpha = 3.64$	0.352	3.464	3.537	4.38

[a]The "effective bond length" for model I was chosen to be 0.923 Å. For all other models, the true bond length, 1.098 Å, was used.

Table III. The considerable improvement in the quality of fit was achieved mainly by the now correct ordering of the optically active modes at Γ, see Table I, although improvements were also noted in the ease with which this model obeyed the two constraints. Detailed study of the calculated values indicates that an effective bond length about 20% less than 1.098 Å would probably provide the best possible fit to all the results, with a χ value rather less than 2. It is very likely that equally satisfactory fits could also be achieved with the Buckingham-type interatomic potential in conjunction with a similar reduction in effective bond length.

The parameters of model I were also used to calculate the dispersion curves in the high-symmetry directions. The calculations were done in two steps in order to incorporate the concept of the effective bond length. First the dynamical matrix was diagonalized for a short-bond model with the forces acting at the atomic centers. The frequencies were then normalized corresponding to the amount of librational character, as determined from the eigenvectors, so that they corresponded to the correct moment of inertia. At the high-symmetry points where the actual comparison with experiments is made the separation in librational and translational character is complete and this calculation procedure introduces no error. Indeed, this approximation is numerically satisfactory except in regions of complicated multiple "crossings and anticrossings," for example, halfway along the Δ direction, near 5 meV. The peculiar shapes of the curves here should not be taken too literally. In any event there is little hope of verifying these curves experimentally because of their complexity. All the calculated curves are shown in Fig. 5, together with observed frequencies along these directions, mainly belonging to the acoustic branches. Furthermore, the expected neutron scattering at the Γ, R, and M points in various zones was calculated on the basis of the model eigenvalues and eigenvectors. The comparison with the actual observations at a series of R points is shown in Fig. 2. The full curves are the calculated response taking into account resolution, monitor sensitivity, background, and estimated intrinsic widths. The same scale factor, temperature factor,[17] and background were used for all scans.

V. DISCUSSION

It is apparent from the comparison between the experimental observations and the model calculations, as illustrated by Figs. 2 and 5, and Table III, model I, that the lattice modes in the α-phase of solid nitrogen at 15 K are very well described by a potential function of the form given in Eqs. (1)–(4), provided that a reduced "effective" bond length is chosen about 15–20% shorter than the true molec-

FIG. 5. Dispersion curves for α-N_2 at 15 K, for intermolecular modes propagating along the [001], [110], and [111] directions of high symmetry. The triangles and circles are experimental measurements, while the solid and dashed curves are theoretical calculations based on model I, Table III. The group-theoretical labels refer to an assumed $Pa3$ structure.

ular bond length.

Other possible variations of the potential function, such as reduction of the Lennard-Jones parameter n from 12 to 10, or small changes in the exponent α, Eq. (3), seem to be much less effective than a reduction of the bond length, as far as fitting the observed normal-mode frequencies is concerned. We note that all the models indicate a somewhat lower electric quadrupole moment QM ($\sim 1.1 \times 10^{-26}$ esu cm^2) for the nitrogen molecule than the experimental value $[(1.4 \pm 0.1) \times 10^{-26}$ esu cm$^2)]$.[31,32] In fact, we should regard QM as a basic parameter instead of the point charge z, since the latter simply increases, as we reduce the bond length, so as to keep QM fairly constant. This is seen in Table IV, which compares two of the present Lennard-Jones models with four previous models taken from the literature. The value QM = 1.52 of QM refers to an earlier determination,[31] now believed to be too high. (The sign of QM is actually negative, corresponding to a net negative charge on the axis of the molecule, at or near each nitrogen atom. The phonon frequencies and total energy depend on Z^2, however.) It is interesting to note that in the present model the electrostatic interactions are comparable to but rather less impor-

tant than the shorter-range terms in the crystal potential. This result may appear to contradict the findings of Jacobi and Schnepp,[10] whose quantum-mechanical calculations of the Raman-active modes based on electric quadrupole interactions gave an excellent fit to the three observed frequencies. However, since these calculations were for 10 nearest-neighbor shells of point quadrupoles, with the observed moment 1.4×10^{-26} esu cm^2, as compared with our complete summation over extended point-charge distributions having a 20% lower moment, it is difficult to make quantitative comparisons. In any case, it is quite possible that a limited selection of the data (e.g., the *gerade* modes only) may be satisfactorily described by

TABLE IV. Comparison of various Lennard-Jones models for α-N_2. Units: Q, 10^{-26} esu; A, 10^2 kcal/mole Å (Ref. 6); D, 10^5 kcal/mole Å (Ref. 12).

Ref.	Author	Q	A	D
5	Schnepp and Ron	0	5.360	7.658
3	Anderson *et al.*	1.26	5.029	11.563
6	Goodings and Henkelman	1.52	4.911	6.034
32	Raich *et al.*	1.4/1.52	4.829	12.349
	model I, this paper	1.112	3.983	5.970
	model II, this paper	1.022	3.575	4.544

several very different models, many of which could be rejected simply by testing them against *all* the available data.

Our calculation is quasiharmonic and, in principle, we could determine the effective potential, i.e., the parameters A, B, and QM, at various temperatures. A more satisfactory approach to the analysis of the temperature dependence has been outlined by Raich *et al.*[33] They have performed a self-consistent phonon calculation on the basis of a model similar to ours but which does not include the electric quadrupole interactions. Accordingly their calculated frequencies are only in fair agreement with our observations. However, the relative temperature dependences are quite well predicted by their approach. This is illustrated in Fig. 4, where the curve represents their calculated behavior of the E_g mode normalized to the observed frequency at 8 K. On the other hand, the singular behavior of the T_g mode does not follow from the self-consistent calculations. An additional source of broadening and renormalization could be an increased molecular disorder in the α-phase as the temperature is raised. Reynolds[34] has estimated such effects for molecular crystals of the halobenzenes and he concludes that in cases where two

or more molecular-ordered structures have comparable free energies and at temperatures where the vacancy concentration is appreciable ($\sim 10^{-3}$) large fluctuations in the local order are to be expected. The existence of the three phases of solid nitrogen suggests that similar considerations may apply here.

Preliminary analysis of our measurements in the β-phase indicates that the potential parameters we have derived from the present work give the right over-all strength of interaction in the hexagonal phase. Thus the potential function may be well suited as the basis for the more detailed model calculations needed to elucidate the microscopic mechanism of the various phase transitions in solid nitrogen. To that end more work is needed both theoretically and experimentally, especially the pressure dependence of the normal modes.

ACKNOWLEDGMENTS

*Present address: On leave from AEK RISØ, DK-4000 Roskilde, Denmark.

†Work at Brookhaven performed under the auspices of the U. S. Atomic Energy Commission.

‡Guest scientist at Brookhaven National Laboratory.

[1]A. Anderson and G. E. Leroi, J. Chem. Phys. **45**, 4359 (1966).

[2]A. Ron and O. Schnepp, J. Chem. Phys. **46**, 3991 (1967); R. V. St. Louis and O. Schnepp, J. Chem. Phys. **50**, 5177 (1969).

[3]A. Anderson, T. S. Sun, and M. C. A. Donkersloot, Can. J. Phys. **48**, 2265 (1970).

[4]P. M. Mathai and E. J. Allin, Can. J. Phys. **49**, 1973 (1971).

[5]O. Schnepp and A. Ron, Discuss. Faraday Soc. **48**, 26 (1969).

[6]D. A. Goodings and M. Henkelman, Can. J. Phys. **49**, 2898 (1971).

[7]J. C. Raich, J. Chem. Phys. **56**, 2395 (1972).

[8]P. V. Dunmore, J. Chem. Phys. **57**, 3348 (1972).

[9]A. B. Harris and C. F. Coll, Solid State Commun. **10**, 1029 (1972).

[10]N. Jacobi and O. Schnepp, J. Chem. Phys. **58**, 3647 (1973).

[11]M. M. Thiery, D. Fabre, M. Jean-Louis, and H. Vu, J. Chem. Phys. **59**, 4559 (1973).

[12]F. Medina and W. B. Daniels, Phys. Rev. Lett. **32**, 167 (1974); J. Chem. Phys. (to be published).

[13]M. Nielsen and K. Carniero, in *Neutron Inelastic Scattering* (I.A.E.A., Vienna, 1972), p. 111; M. Nielsen. Phys. Rev. B **7**, 1626 (1973).

[14]B. M. Powell, G. Dolling, L. Piseri, and C. P. Martel, in Ref. 13, p. 207.

[15]B. N. Brockhouse, in *Inelastic Scattering of Neutrons*

in Solids and Liquids (I.A.E.A., Vienna, 1961), p. 113.

[16]C. A. Swenson, J. Chem. Phys. **23**, 1963 (1955).

[17]A. F. Schuch and R. L. Mills, J. Chem. Phys. **52**, 6000 (1970).

[18]W. E. Streib, T. H. Jordan, and W. N. Lipscomb, J. Chem. Phys. **37**, 2962 (1962).

[19]T. H. Jordan, H. W. Smith, W. E. Streib, and W. N. Lipscomb, J. Chem. Phys. **41**, 756 (1964).

[20]J. Skalyo, Jr. and Y. Endoh, Phys. Rev. B **7**, 4670 (1973).

[21]D. C. Heberlein, E. D. Adams, and T. A. Scott, J. Low Temp. Phys. **2**, 449 (1970).

[22]E. W. Kellermann, Philos. Trans. R. Soc. Lond. A **238**, 513 (1940).

[23]A. J. Kitaigorodskii, J. Chim. Phys. **63**, 8 (1966).

[24]D. E. Williams, J. Chem. Phys. **45**, 3770 (1966); **47**, 4680 (1967).

[25]G. Dolling, B. M. Powell, and G. S. Pawley, Proc. R. Soc. A **333**, 363 (1973).

[26]P. A. Reynolds, J. Chem. Phys. **59**, 2777 (1973).

[27]R. W. G. Wyckoff, *Crystal Structures*, 2nd ed. (Wiley, New York, 1963), Vol. 1.

[28]B. Stoicheff, Can. J. Phys. **32**, 630 (1954).

[29]B. C. Kohin, J. Chem. Phys. **33**, 882 (1960).

[30]W. F. Giauque and J. O. Clayton, J. Am. Chem. Soc. **55**, 4875 (1933).

[31]D. E. Stogryn and A. P. Stogryn, Mol. Phys. **11**, 371 (1966).

[32]A. D. Buckingham, R. L. Disch, and D. A. Dunmur, J. Am. Chem. Soc. **90**, 3104 (1968).

[33]J. C. Raich, N. S. Gillis, and A. B. Anderson (unpublished).

[34]P. A. Reynolds, Mol. Phys. (to be published).